ACS Catalysis

Research Article

Cite This: ACS Catal. 2018, 8, 1485−1489

pubs.acs.org/acscatalysis

Adsorbed Hydroxyl and Water on Ni(111): Heats of Formation by Calorimetry

Wei Zhao, Spencer J. Carey, Zhongtian Mao, and Charles T. Campbell*

Department of Chemistry, University of Washington, Seattle, Washington 98195-1700, United States

ABSTRACT: Adsorbed hydroxyl is a common intermediate in many catalytic reactions on Ni catalysts. The heat of the dissociative adsorption of D_2O onto an O-precovered Ni(111) surface producing adsorbed hydroxyls is measured here by single crystal adsorption calorimetry, with an average value of 67.3 kJ/mol up to 0.23 ML coverage. From this, the enthalpy of formation for adsorbed hydroxyl on Ni(111) and the bond energy of hydroxyl to Ni(111) were estimated to be −278.3 and 314.1 kJ/mol, respectively. The molecular adsorption of D_2O on clean Ni(111) gave an integral heat of 53.6 kJ/mol at 0.5 ML. In comparison to Pt(111), adsorbed hydroxyl binds to Ni(111) 67 kJ/mol more strongly and adsorbed D_2O binds to Ni(111) ∼ 2 kJ/mol more strongly. These energetics help clarify the different catalytic properties of Ni versus Pt, and serve as benchmarks to evaluate the energy accuracy of quantum mechanical methods used in surface chemistry.

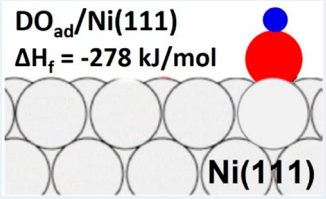

KEYWORDS: *adsorbed hydroxyl, water adsorption, water dissociation, nickel, platinum, Ni(111), adsorption energy, calorimetry, heat of adsorption*

INTRODUCTION

The adsorption and dissociation of water are important elementary steps in numerous important catalytic and electrocatalytic reactions on Ni and other transition metal catalysts, such as the water gas shift reaction, the steam reforming or oxidation of practically any organic molecule, and water splitting.[1−3] Surface hydroxyl is a key intermediate in these reactions. Much work has been devoted to study the interaction of water on clean or oxygen-precovered transition metal surfaces, as summarized in a nice review article.[4] However, those previous experimental studies mainly focused on the adsorption structures and desorption kinetics of adsorbates (molecularly adsorbed water for most cases). Knowledge of the energetics of adsorbed hydroxyl, which is crucial for better understanding catalytic reaction rates, is still lacking. Until now, the heat of formation for surface hydroxyl has only been previously measured on one metal surface, Pt(111), as reported by this group.[5,6] Herein, we report calorimetric measurements of the heat of formation of adsorbed hydroxyl on Ni(111) and find it to be bound ∼67 kJ/mol more strongly than to Pt(111). This helps clarify some of the differences in catalytic properties of Ni versus Pt catalysts.

The adsorption of D_2O on clean Ni(111) and oxygen-precovered Ni(111) were previously studied by temperature-programmed desorption (TPD) and high-resolution electron energy loss (HREEL) spectroscopy.[7,8] Adsorbed hydroxyl was identified as the product of heating D_2O adlayers on oxygen-precovered Ni(111) to 170 K.[7] In our experiments, a molecular beam of D_2O was introduced onto a clean Ni(111) surface and an O-precovered Ni(111) surface at different temperatures. Single crystal adsorption calorimetry (SCAC) was employed to directly measure the heats of D_2O adsorbed onto the surfaces, molecularly and dissociatively, allowing us for the first time to extract the enthalpy of formation and the bond enthalpy of adsorbed hydroxyl on Ni(111). These energetic values are of importance for all catalytic reactions involving water and hydroxyl on nickel-related catalysts, and also serve as benchmarks for validating the energy accuracy of theoretical estimates of the stability of −OH and oxygenates (e.g., $-OCH_3$) bound to Ni catalyst surfaces.

EXPERIMENTAL SECTION

The Ni(111) sample used here is a 1 μm thick single-crystal foil, supplied by Jacques Chevallier at Aarhus University in Denmark, and the surface was cleaned by cycles of Ar^+ ion sputtering and annealing. The experiments were performed in an ultrahigh vacuum (UHV) chamber (base pressure <2 × 10^{-10} mbar), designed for SCAC and surface analysis, as described previously.[9,10] A detailed description of the experimental principles and implementation of the molecular beam flux, sticking probability, and heat measurements can be found elsewhere.[9−11] Briefly, the clean and O-precovered Ni(111) surface, held at different temperatures, was exposed to a pulsed molecular beam of D_2O, and the heat of adsorption and sticking probability were recorded simultaneously for each pulse. The atomic oxygen-precovered surface was prepared by exposing the clean Ni(111) surface to O_2 at cryogenic conditions (100−170 K) as described in the literature,[12−14] and the coverage of preadsorbed oxygen was measured by X-ray photoelectron spectroscopy (XPS). The heat of D_2O adsorption was detected using a pyroelectric heat detector pressed against the back of the Ni(111) crystal, and the sticking probability was measured with the quadrupole mass spectrometer (QMS) using the King and Wells method.[15] The

Received: November 26, 2017
Revised: January 5, 2018
Published: January 9, 2018

DOI: 10.1021/acscatal.7b04041
ACS Catal. 2018, 8, 1485−1489

beam was created by expanding ~2 mbar of D_2O through a microchannel array and then collimated through a series of five liquid nitrogen cooled orifices, and chopped into 102 ms pulses every 5 s with a rotating chopper blade.

We define coverage of D_2O molecules that adsorb onto the surface irreversibly (whether molecularly adsorbed or dissociatively adsorbed) in units of monolayers (ML) where 1 ML = 1.86×10^{19} species per m^2, which is the surface atom density of Ni(111). A typical molecular beam flux gives 0.008 ML (~1.37×10^{12} molecules within the beam diameter of ~4 mm) per D_2O pulse.

RESULTS

Sticking Probability. We measure the long-term sticking probability and the short-term sticking probability. The long-term sticking probability is the probability that a gas molecule strikes the sample surface, sticks, and remains until the next gas pulse starts ~5 s later. It is used to calculate the increase in adsorbate coverage due to that pulse. The short-term sticking probability is the probability that a gas molecule strikes the sample surface, sticks, and remains at least throughout the time window of our heat measurement (i.e., the first 102 ms). This is used to calculate the number of moles of gas-phase reactant that contribute to the measured heat of adsorption. Figure 1

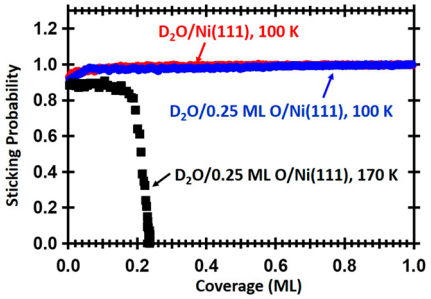

Figure 1. Long-term sticking probabilities of D_2O adsorption on clean Ni(111) and oxygen-precovered Ni(111) as a function of total D_2O coverage. Red curve: D_2O molecularly adsorbed on clean Ni(111) at 100 K; Blue curve: D_2O molecular adsorption on 0.25 ML oxygen-precovered Ni(111) at 100 K; Black curve: D_2O dissociative adsorption on 0.25 ML oxygen-precovered Ni(111) at 170 K.

shows the long-term sticking probabilities of D_2O on clean Ni(111) at 100 K and on 0.25 ML O-precovered Ni(111) at 100 and 170 K, respectively. The coverage reported here and elsewhere represents the D_2O permanently adsorbed, regardless of the products produced. At 100 K, the D_2O molecularly adsorbs on clean Ni(111) and O-precovered Ni(111) to form a multilayer (see the Discussion below). Both the long-term (red and blue curves in Figure 1) and short-term (not shown here) sticking probabilities are almost unity at multilayer coverage. The initial sticking probabilities are ~0.92 for both surfaces and slightly increase as more D_2O molecules are adsorbed, indicating a precursor-mediated adsorption mechanism. At 170 K on 0.25 ML O-precovered Ni(111), D_2O dissociates and forms adsorbed hydroxyls, as discussed below. At 170 K, the long-term sticking probability starts at ~0.9 and quickly decreases to zero between 0.18 and 0.23 ML, while the short-term sticking probability remains high (>0.85, not shown here). This indicates that the adsorption of D_2O on Ni(111) precovered with 0.25 ML O saturates at ~0.23 ML at 170 K, but that D_2O still transiently adsorbs with high probability on that saturated adlayer and desorbs again slowly (but before the next pulse arrives 5 s later).

Heats of Molecular Adsorption on clean and O-precovered Ni(111). In this paper, the term "heat of adsorption" is defined as the negative of the differential standard molar enthalpy change for the adsorption reaction, with the gas and the sample surface being at the same temperature. As described previously, this requires a small enthalpy correction on the measured heat since the gas molecule's enthalpy at this temperature is slightly different from the actual experimental molecular beam conditions.[11,16]

According to the literature, water adsorbs molecularly on clean Ni(111), and TPD studies show that the multilayers desorb at 150 K and the monolayer desorbs at 165 K.[7,8,17,18] Hodgson et al.[4,17] observed 2D wetting islands with a $(2\sqrt{7} \times 2\sqrt{7})R19°$ structure upon water molecular adsorption on Ni(111) in the submonolayer region. The islands grow bigger until saturation of the first adlayer, showing a $(2\sqrt{7} \times 2\sqrt{7})R19°$ structure which can easily change into the $(\sqrt{3} \times \sqrt{3})R30°$ structure by the impact of the LEED electron beam. They proposed that this $(2\sqrt{7} \times 2\sqrt{7})R19°$ structure is a distorted hexagonal water network stabilized by hydrogen bonds wherein one unit cell contains 18 water molecules per 28 Ni atoms, giving a coverage of monolayer water on Ni(111) of ~0.64 ML.[17] Very recently, Thürmer et al.[19] employed STM to find that water forms ~1 nm wide 2D islands on Ni(111) up to 0.5 ML and the continuous 2D wetting layer emerges only above 0.5 ML. Reanalyzing the $(2\sqrt{7} \times 2\sqrt{7})R19°$ monolayer structure with STM and DFT, they offered a more likely interpretation of its structure as involving 16 water molecules per 28 Ni atoms, giving a coverage of ~0.57 ML, consistent with our results below. After the first monolayer is completed, the second layer grows on top of the first and 3D ice particles nucleate and grow above the second layer until amorphous ice-like multilayers are formed.[19] For O-precovered Ni(111), water molecularly adsorbs on the surface below ~150 K but desorbs at higher temperature compared to that for clean Ni(111).[7]

Figure 2 shows the evolution of this differential heat of adsorption of D_2O on clean Ni(111) (in red) and O-precovered Ni(111) (in blue) as a function of the coverage of adsorbed D_2O at 100 K, where D_2O builds up multilayers for both surfaces and the heats represent molecular adsorption. For clean Ni(111) at 100 K, the differential heat of adsorption starts at 54.1 kJ/mol and slightly increases up to ~0.3 ML, implying

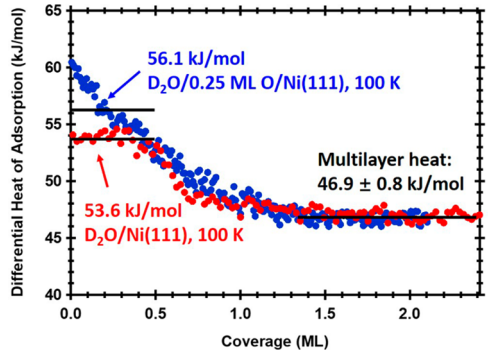

Figure 2. Differential heats of D_2O molecular adsorption on clean Ni(111) and 0.25 ML oxygen-precovered Ni(111), both at 100 K, as a function of total D_2O coverage. They both give the same multilayer heat at 46.9 ± 0.8 kJ/mol, however, O-precovered Ni(111) gives 2.5 kJ/mol higher integral heat for the first layer.

DOI: 10.1021/acscatal.7b04041
ACS Catal. 2018, 8, 1485−1489

an attractive force between adsorbed water molecules at low coverage. From 0.3 to 0.5 ML, the heat slightly decreases again but remains almost constant from 0 to ~0.5 ML. After 0.5 ML, the heat decreases quickly to ~48.2 kJ/mol until ~0.7 ML and more slowly to 46.9 ± 0.8 kJ/mol as D_2O multilayers are built up. This evolution of heats versus coverage of adsorbed water can be interpreted with the literature studies summarized above,[17,19] i.e., water initially forms small 2D islands on Ni(111) up to 0.5 ML, where the 2D islands merge into a continuous monolayer with $(2\sqrt{7} \times 2\sqrt{7})R19°$ structure, corresponding to ~0.57 ML ideally. This ideal monolayer coverage is very close to the midpoint of the rapid drop in heat from its monolayer heat to the multilayer heat, at 0.4 to 0.7 ML in Figure 2. We attribute the width of this drop to the heterogeneity in local coverages. (That is, this drop is a broadened step function centered near 0.57 ML.) The integral heat of molecular adsorption of D_2O on Ni(111) is 53.6 kJ/mol for the most stable adlayer at 0.5 ML, which probably best reflects the heat of the $(2\sqrt{7} \times 2\sqrt{7})R19°$ structure of 0.57 ML, due to the strong contributions from the lower heat at multilayer patches by 0.57 ML in Figure 2. In the previous calorimetric study of D_2O on Pt(111) by this group,[20] we found a very similar heat versus coverage, with an integral heat of 51.3 kJ/mol at 0.5 ML. Thus, water molecularly adsorbs on Ni(111) ~ 2.3 kJ/mol more strongly than on Pt(111).

The multilayer heat for D_2O on Ni(111) is 46.9 ± 0.8 kJ/mol, consistent with the previous calorimetric data for D_2O on Pt(111).[20] We can compare the measured monolayer and multilayer heats of D_2O on Ni(111) to the previous TPD studies (the maximum desorption peaks for the monolayer and multilayer are at 160 and 170 K, respectively).[7,8] To do this, the prefactors for D_2O desorption are estimated to be 3.05×10^{14} s^{-1} at 170 K (monolayer desorption) and 2.87×10^{14} s^{-1} at 160 K (multilayer desorption), respectively, following the entropy method developed by Campbell and Sellers[21,22] using the standard gas-phase entropy of D_2O of 181.26 J/(mol K) at 170 K and 178.89 J/(mol K) at 160 K.[23,24] The activation energies are estimated to be 46.4 kJ/mol for the multilayer desorbed at 160 K and 49.4 kJ/mol for the monolayer desorbed at 170 K using the simple first-order Redhead analysis.[21] In comparison to the calorimetric heats, $^1/_2RT$ has to be added to the TPD values, giving 47.1 kJ/mol as the multilayer heat and 50.1 kJ/mol as the monolayer heat, showing a quite good agreement with our calorimetric heat values (46.9 and 53.6 kJ/mol, respectively).

As the literature has shown, D_2O molecularly adsorbs on O-precovered Ni(111) at 100 K.[7,18,25] Figure 2 shows that the integral heat at 100 K is 56.1 kJ/mol at 0.5 ML of adsorbed D_2O for the Ni(111) surface precovered with 0.25 ML O, which is 2.5 kJ/mol higher than that of D_2O on clean Ni(111). This is in line with the literature; that is, the attractive force between adsorbed D_2O and O makes the coadsorbed molecules more stable on O-precovered Ni(111).[18,25] We also did calorimetry experiments for D_2O adsorption on oxygen-precovered Ni(111) at 120 K, and it showed nearly the same evolution of heat versus coverage as at 100 K in Figure 2, indicating molecular adsorption at 120 K as well.

Heat of Dissociative Adsorption on O-Precovered Ni(111). A recent HREEL and TPD study[7] unambiguously identified the formation of adsorbed hydroxyl species on Ni(111) by heating coadsorbed water and O on Ni(111) to 170 K, which was also observed by Madey and Netzer[26] previously. However, Ni(111) is thought to not form the hydroxyl–water complex formed on Pt(111) when water dissociatively adsorbs on the O-precovered surface.[4,27,28] The spectra observed in that HREEL and TPD study were interpreted as due to pure hydroxyl without coadsorbed water on Ni(111).[7] This is because hydroxyl binds at 3-fold hollow sites much more strongly than at other sites on Ni(111),[29−31] and the O–H axis is predicted to be only slightly tilted from the surface normal,[29] which does not allow the hydroxyl to form hydrogen bonds with water on Ni(111). (Such hydrogen bonds require the O–H axis to be more parallel to the surface.) In contrast, hydroxyl binds at top sites on Pt(111) with its O–H axis orientated nearly parallel to the surface, which facilitates the formation of hydroxyl–water complex.[27] Thus, the dissociative adsorption of D_2O on O-precovered Ni(111) has been attributed to the reaction 1:

$$D_2O_g + O_{ad} \rightarrow 2OD_{ad} \quad (1)$$

Figure 3 shows the evolution of this differential heat of adsorption of D_2O on 0.25 ML O precovered Ni(111) as a function of the coverage of adsorbed D_2O at 170 K. It shows the differential heat starts from ~70.0 kJ/mol, then deceases to ~65.7 kJ/mol at the saturation coverage of 0.23 ML. The integral heat is depicted as the red dash curve in Figure 3, and it is 67.3 kJ/mol at saturated coverage. This integral heat is significantly higher than that of molecularly adsorbed D_2O on 0.25 ML O precovered Ni(111) at 100 K (56.1 kJ/mol), which supports interpretation as the dissociative adsorption of D_2O on O-precovered Ni(111) at 170 K, but molecular at 100 K. At 170 K, the saturation coverage of adsorbed D_2O (~0.23 ML) is close to the coverage of preadsorbed O (~0.25 ML), indicating that close to $^1/_2$ ML of adsorbed hydroxyl is produced on Ni(111) at saturation (i.e., one $D_2O_g + O_{ad}$ produces two OD_{ad}). In comparison, we also performed calorimetric measurements of D_2O adsorption on clean Ni(111) at 170 K (not shown here), showing that only a tiny amount of D_2O (~0.006 ML) can be adsorbed at this temperature, with a heat value (~54 kJ/mol) very similar to that for molecular adsorption on clean Ni(111) at 100 K. This low saturation coverage of water on clean Ni(111) at 170 K in our experiment is in line with the TPD study, where the peak maximum for desorption of water from clean Ni(111) is ~170 K.[7,8] Therefore, the larger measured heat at 170 K (67.3 kJ/mol) on O-precovered Ni(111) is assigned to the heat of dissociative

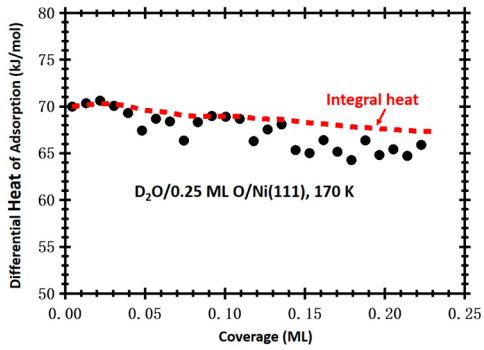

Figure 3. Differential heat of D_2O dissociative adsorption on 0.25 ML O-precovered Ni(111) at 170 K as a function of total D_2O coverage. The red dash curve shows the integral heat, giving 67.3 kJ/mol at saturation.

DOI: 10.1021/acscatal.7b04041
ACS Catal. 2018, 8, 1485−1489

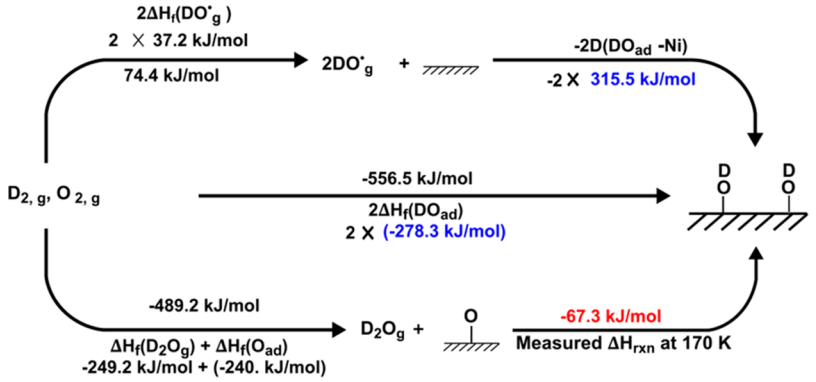

Figure 4. Thermodynamic cycles used to determine the heat of formation of hydroxyl adsorbed on Ni(111) from the calorimetric *integral* heat of dissociative D_2O adsorption on the O-predosed surface at 170 K and ~1/4 ML (shown in red). The top right-hand step shows the enthalpy to form adsorbed hydroxyl from gas-phase hydroxyl radical, which provides an estimate of the bond enthalpy of hydroxyl to Ni(111). Enthalpies in black are literature values as referenced in the text.

adsorption of D_2O to make adsorbed hydroxyls, also consistent with this much higher saturation coverage.

DISCUSSION

Enthalpies of Formation of Adsorbed Hydroxyl on Ni(111). Using available literature values for the heats of formation of various gas-phase and adsorbed species, the enthalpies of formation of adsorbed hydroxyl and the DO-Ni(111) bond enthalpy can be extracted from the heats of D_2O adsorption onto Ni(111) measured by calorimetry, shown as the thermodynamic cycles in Figure 4.

The bottom route in the cycle begins with elements in their standard states, along the bottom-left arrow forming gas-phase D_2O with the standard enthalpy of formation $\Delta H_f(D_2O_g)$ = −249.2 kJ/mol[23] and $^1/_4$ ML O_{ad} on Ni(111) with enthalpy of formation $\Delta H(O_{ad})$ = −240.0 kJ/mol.[16,32,33] The bottom-right arrow then represents the dissociative adsorption process, which we measured by calorimetry. This is the *integral* enthalpy of dissociative adsorption of one D_2O molecule on O_{ad}-Ni(111) leading to two OD_{ad} at 170 K, −67.3 kJ/mol at ~$^1/_4$ ML (0.23 ML) of dissociatively adsorbed D_2O. While this heat of adsorption represents an exothermic process and thus has negative reaction enthalpy in the thermodynamic cycle, the heats were shown as positive values in Figure 3 to represent the corresponding heat release (and thus they represent the negative of reaction enthalpies there).

The middle route in the cycle of Figure 4 is the direct conversion of standard-state elements to the adsorbed products, which is energetically equivalent to the bottom route. The standard enthalpy of formation of adsorbed hydroxyl, $\Delta H_f(OD_{ad})$, is thus determined to be −278.3 kJ/mol.

The top route of the thermodynamic cycle allows for a similar calculation of the bond enthalpy between adsorbed hydroxyl and the Ni(111) surface. The top left arrow takes the standard-state elements to gas-phase hydroxyl radical by means of its enthalpy of formation, +37.2 kJ/mol.[23] This allows for the calculation of the top right arrow enthalpy change, representing the negative of the adiabatic DO_{ad}-Ni(111) bond dissociation enthalpy to make DO^*_g and Ni(111), to be −315.5 kJ/mol. Thus, +315.5 kJ/mol is the enthalpy arising from breaking the O−Ni bond between adsorbed hydroxyl and the Ni(111) surface, or $D(DO_{ad}\text{-Ni(111)})$.

Comparison to DFT Calculations. The bond enthalpy of hydroxyl binding to Ni(111) extracted in this calorimetry work is 315.5 kJ/mol at 170 K for the coverage of ~$^1/_2$ ML, thus the bond energy of hydroxyl to Ni(111) is 314 kJ/mol, obtained by subtracting *RT*. This experimentally measured energy value is compared to five DFT calculated bond energies of hydroxyl on Ni(111) at zero K, shown in Table 1. Except ref.[34] using GGA-RPBE, the other four DFT values (using GGA-PBE or GGA-PW91) differ from the experimental value by −13 kJ/mol to +16 kJ/mol. This is fairly good agreement considering the zero-point energy and heat-capacity corrections are not included in the comparison and the possible error in the DFT energy of gaseous hydroxyl radical. It is interesting that RPBE does so much more poorly than the PBE and PW91 functionals.

Table 1. Comparison of Present Calorimetrically Measured Bond Energy of Hydroxyl to the Ni(111) Surface with DFT Calculated Values of the Most Stable Sites for Hydroxyl Binding to Ni(111)

cverage	functional or method	bond energy (kJ/mol)	ref
~1/2 ML	calorimetry	314	this paper
DFT Methods			
1/4 ML	GGA-RPBE	241	34
1/9 ML	GGA-PBE	330.	35
1/4 ML	GGA-PBE	303	31
1/9 ML	GGA-PW91	301	36
1/6 ML	GGA-PBE	308	37

Comparison to Pt(111). Previous calorimetric measurements have determined the bond energy for hydroxyl to Pt(111) to be 246.7 kJ/mol (the bond enthalpy of 248 kJ/mol at 150 K subtracted by *RT*).[5,6] This is 67.4 kJ/mol weaker than the bond energy of 314.1 kJ/mol found here for hydroxyl to Ni(111). This is expected, since Ni is well-known to be more oxophyllic than Pt. Moreover, our previous calorimetry studies showed that bidentate formate also binds to Ni(111) more strongly than to Pt(111).[38,39] Also, DFT studies give a larger bonding energy for hydroxyl to Ni(111) (241 to 330 kJ/mol for isolated OH_{ad} in Table 1) than to Pt(111) (179 kJ/mol for isolated OH_{ad} and 217 kJ/mol for OH_{ad} within $(H_2O{-}OH)_{ad}$ complex[6]).

These experimentally measured differences in the strength of oxygenated intermediates binding to Ni and Pt through O atoms help us to understand differences in the catalytic properties of these two metals. For example, given that alkyl groups such as methyl also bond more strongly to Ni(111)

DOI: 10.1021/acscatal.7b04041
ACS Catal. 2018, 8, 1485−1489

than Pt(111),[40] reactions that require C−O bond cleavage in molecules such as alcohols and ethers should proceed more rapidly on Ni than Pt catalysts since both products (−OR or −OH and $-CR_x$) bond more strongly to Ni than Pt. Conversely, C−O bond-forming reactions should be slower on Ni than on Pt.

CONCLUSIONS

The energetics of D_2O adsorbed on Ni(111), molecularly and dissociatively, were directly measured by calorimetry. The integral heat of adsorption of molecularly adsorbed D_2O on Ni(111) is 53.6 kJ/mol at 0.5 ML and 53.1 kJ/mol at 0.64 ML. The integral heat of dissociative adsorption of D_2O on O-predosed Ni(111) at 170 K to make two surface −ODs is 67.3 kJ/mol at 0.23 ML, giving the enthalpy of formation of hydroxyl (−OD) on Ni(111) to be −278.3 kJ/mol and the bond dissociation enthalpy of hydroxyl from Ni(111) to be 315.5 kJ/mol. Hydroxyl binds to Ni(111) ∼67 kJ/mol more strongly than to Pt(111), in agreement with the greater oxophilicity of Ni versus Pt. These precisely measured energetic values are crucial to understand the catalytic activity differences between Ni and Pt in reactions involving adsorbed oxygenates.

AUTHOR INFORMATION

Corresponding Author

*E-mail: charliec@uw.edu. Tel.: 206-616-6085.

ORCID

Wei Zhao: 0000-0001-5407-6164

Charles T. Campbell: 0000-0002-5024-8210

Notes

The authors declare no competing financial interest.

ACKNOWLEDGMENTS

The authors acknowledge support for this work by the National Science Foundation under Grant No. CHE-1665077.

REFERENCES

(1) Hwang, K.-R.; Lee, C.-B.; Park, J.-S. *J. Power Sources* **2011**, *196*, 1349−1352.
(2) Rostrup-Nielsen, J. R. *J. Catal.* **1973**, *31*, 173−199.
(3) Yan, Y.; Xia, B. Y.; Zhao, B.; Wang, X. *J. Mater. Chem. A* **2016**, *4*, 17587−17603.
(4) Hodgson, A.; Haq, S. *Surf. Sci. Rep.* **2009**, *64*, 381−451.
(5) Lew, W.; Crowe, M. C.; Karp, E.; Lytken, O.; Farmer, J. A.; Árnadóttir, L.; Schoenbaum, C.; Campbell, C. T. *J. Phys. Chem. C* **2011**, *115*, 11586−11594.
(6) Karp, E. M.; Campbell, C. T.; Studt, F.; Abild-Pedersen, F.; Nørskov, J. K. *J. Phys. Chem. C* **2012**, *116*, 25772−25776.
(7) Shan, J.; Kleyn, A. W.; Juurlink, L. B. F. *ChemPhysChem* **2009**, *10*, 270−275.
(8) Shan, J.; Aarts, J. F. M.; Kleyn, A. W.; Juurlink, L. B. F. *Phys. Chem. Chem. Phys.* **2008**, *10*, 2227−2232.
(9) Ajo, H. M.; Ihm, H.; Moilanen, D. E.; Campbell, C. T. *Rev. Sci. Instrum.* **2004**, *75*, 4471−4480.
(10) Lew, W.; Lytken, O.; Farmer, J. A.; Crowe, M. C.; Campbell, C. T. *Rev. Sci. Instrum.* **2010**, *81*, 024102.
(11) Lytken, O.; Lew, W.; Harris, J. J. W.; Vestergaard, E. K.; Gottfried, J. M.; Campbell, C. T. *J. Am. Chem. Soc.* **2008**, *130*, 10247−10257.
(12) Zion, B. D.; Hanbicki, A. T.; Sibener, S. J. *Surf. Sci.* **1998**, *417*, L154−L159.
(13) Li, W.; Stirniman, M. J.; Sibener, S. J. *J. Vac. Sci. Technol., A* **1995**, *13*, 1574−1578.
(14) Stirniman, M. J.; Li, W.; Sibener, S. J. *J. Chem. Phys.* **1995**, *103*, 451−460.
(15) King, D. A.; Wells, M. G. *Surf. Sci.* **1972**, *29*, 454−482.
(16) Silbaugh, T. L.; Campbell, C. T. *J. Phys. Chem. C* **2016**, *120*, 25161−25172.
(17) Gallagher, M. E.; Haq, S.; Omer, A.; Hodgson, A. *Surf. Sci.* **2007**, *601*, 268−273.
(18) Pache, T.; Steinrück, H. P.; Huber, W.; Menzel, D. *Surf. Sci.* **1989**, *224*, 195−214.
(19) Thürmer, K.; Nie, S.; Feibelman, P. J.; Bartelt, N. C. *J. Chem. Phys.* **2014**, *141*, 18C520.
(20) Lew, W.; Crowe, M. C.; Karp, E.; Campbell, C. T. *J. Phys. Chem. C* **2011**, *115*, 9164−9170.
(21) Campbell, C. T.; Sellers, J. R. V. *J. Am. Chem. Soc.* **2012**, *134*, 18109−18115.
(22) Campbell, C. T.; Sellers, J. R. V. *Chem. Rev.* **2013**, *113*, 4106−4135.
(23) Chase, M. W. *NIST-JANAF Thermochemical Tables*. 4th ed.; Monograph: J. Phys. Chem. Ref. Data; NIST, 1998; Vol. 9, p 1951.
(24) Yaws, C. L. *Yaws' Handbook of Thermodynamic and Physical Properties of Chemical Compounds: Physical, Thermodynamic and Transport Properties for 5,000 Organic Chemical Compounds*. McGraw-Hill, 2003.
(25) Nakamura, M.; Tanaka, M.; Ito, M.; Sakata, O. *J. Chem. Phys.* **2005**, *122*, 224703.
(26) Madey, T. E.; Netzer, F. P. *Surf. Sci.* **1982**, *117*, 549−560.
(27) Clay, C.; Haq, S.; Hodgson, A. *Phys. Rev. Lett.* **2004**, *92*, 046102.
(28) Held, G.; Clay, C.; Barrett, S. D.; Haq, S.; Hodgson, A. *J. Chem. Phys.* **2005**, *123*, 064711.
(29) Yang, H.; Whitten, J. L. *Surf. Sci.* **1989**, *223*, 131−150.
(30) Yang, H.; Whitten, J. L. *Surf. Sci.* **1997**, *370*, 136−154.
(31) Pozzo, M.; Carlini, G.; Rosei, R.; Alfè, D. *J. Chem. Phys.* **2007**, *126*, 164706.
(32) Stuckless, J. T.; Wartnaby, C. E.; Al-Sarraf, N.; Dixon-Warren, S. J. B.; Kovar, M.; King, D. A. *J. Chem. Phys.* **1997**, *106*, 2012−2030.
(33) Brown, W. A.; Kose, R.; King, D. A. *Chem. Rev.* **1998**, *98*, 797−832.
(34) Blaylock, D. W.; Ogura, T.; Green, W. H.; Beran, G. J. O. *J. Phys. Chem. C* **2009**, *113*, 4898−4908.
(35) Zhu, Y.-A.; Chen, D.; Zhou, X.-G.; Yuan, W.-K. *Catal. Today* **2009**, *148*, 260−267.
(36) Phatak, A. A.; Delgass, W. N.; Ribeiro, F. H.; Schneider, W. F. *J. Phys. Chem. C* **2009**, *113*, 7269−7276.
(37) Zhou, Y.-H.; Lv, P.-H.; Wang, G.-C. *J. Mol. Catal. A: Chem.* **2006**, *258*, 203−215.
(38) Silbaugh, T. L.; Karp, E. M.; Campbell, C. T. *J. Am. Chem. Soc.* **2014**, *136*, 3964−3971.
(39) Zhao, W.; Carey, S. J.; Morgan, S. E.; Campbell, C. T. *J. Catal.* **2017**, *352*, 300−304.
(40) Carey, S. J.; Zhao, W.; Frehner, A.; Campbell, C. T.; Jackson, B. *ACS Catal.* **2017**, *7*, 1286−1294.

DOI: 10.1021/acscatal.7b04041
ACS Catal. 2018, 8, 1485−1489